Robust security constrained optimal power flow considering load and wind power generation uncertainties by applying Taguchi method

SARA-SADAT GHASEMI[1] **AND HAMDI ABDI**[1,*]

[1] *Electrical Engineering Department, Razi University, Kermanshah, Iran*
[*] *Corresponding author: hamdiabdi@razi.ac.ir*

Manuscript received 13 March, 2020; revised 21 May, 2020, accepted 04 June, 2020. Paper no. JEMT-2003-1233.

With the increased use of wind power in power systems, the necessity of revision of conventional deterministic approaches is indisputable. Presenting new and effective methods based on uncertainty modeling is greatly emphasized. In this paper, a new method for investigating the robust security constrained-optimal power flow (RSCOPF) is proposed, which is not only able to comply with security constraints but also robust to the uncertainty of electrical demand loads and wind power generation. The proposed approach is based on the definition of uncertain loads and wind power generation and uses the Taguchi orthogonal array technique (TOAT) , for the first time, a technique which is adopted to solve the RSCOPF by applying the alternating current power flow (ACPF) and particle swarm optimization (PSO) algorithm. Also, some security analyses are presented to introduce the most critical lines and generation units whose loss imposes the highest operating costs on the network. The case study simulation on the IEEE 14-bus system using MATLAB software demonstrates the ability of the proposed algorithm.

keywords: *Taguchi orthogonal arrays technique, AC optimal power flow, Security-constrained, Uncertainty, Robust.*

http://dx.doi.org/10.22109/jemt.2020.223364.1233

NOMENCLATURE

Acronyms

ACO Ant Colony Optimization
ACOPF AC Optimal Power Flow
ACPF AC Power Flow
ADMM Alternating Direction Method of Multipliers
BD Benders Decomposition
CC Corrective Control
CE Cross Entropy
CVaR Conditional value-at-risk
DCOPF DC Optimal Power Flow
DCPF DC Power Flow
DEA Differential Evolution Algorithm
DTR Dynamic Thermal Rating
EP Evolutionary Programming
FAAPO Fuzzy Adaptive Artificial Physics Optimization
GSF Generation Shift Factor
HESS Hybrid Energy Storage Systems
hC-DEEPSO hybrid Canonical DE-Particle Swarm Optimization
IGDT Information Gap Decision Theory
IP Interior-Point
LSFs Linear Sensitivity Factors
MBFA Modified Bacteria Foraging Algorithm
MINLP Mixed-Integer Non-Linear Programming
OPF Optimal Power Flow
PC Preventive Control
POPF Probabilistic Optimal Power Flow
PSO Particle Swarm Optimization
RSCOPF Robust Security Constrained Optimal Power Flow
SOC State of Charge
TOAT Taguchi Orthogonal Array Technique
USCOPF Uncertain Security Constrained Optimal Power Flow

Symbols and parameters

P_{Gi}, Q_{Gi} The output active and reactive powers of unit i
P The bus injection power vector

$\tilde{P}$ The probabilistic bus injection power vector

P_G The vector of generation power

P_{Load} The load vector

$\tilde{P}_{Load}$ The probabilistic load vector

P_{Res} Power generation vector by wind power plants

$\tilde{P}_{Res}$ The vector of probabilistic power generation by wind power plants

$\underline{P}_G, \overline{P}_G$ The vectors of the lower, and upper limits of active generation power

$\underline{Q}_G, \overline{Q}_G$ The vectors of the lower, and upper limits of reactive generation power

P_i The injection power for bus i

$|V_i|$ The per-unit voltage magnitude of bus i

$|\underline{V}_i|, |\overline{V}_i|$ The minimum, and maximum per-unit voltage magnitude of bus i

P_L The power flow of line L between buses i, and j

$\underline{P}_{Line}$ The vector of the lower limit of transmission power

$\overline{P}_{Line}$ The vector of the upper limit of transmission power

ΔP_{Line} The vector of change in the power flow of lines

ΔP_i The change in the injection power of unit i

P_{Line} Power vector of lines

H The vector of generation shift factors

H_{Res}, H_{Load}, H_G Columns of the matrix H

a_i, b_i, c_i The cost coefficients for the i-th unit

h_{Li} The generation shift factors

Y_j The performance index

f_{jL} The power flow on line L obtained from the power flow calculations regarding the experiment j

f_L^* The nominal power flow on line L

G_{ij}, B_{ij} The conductance and susceptance value for line L, connected between buses i and j

n_{ij} The per-unit transformer tap-ratio located at branch i-j

$\underline{n}_{ij}, \overline{n}_{ij}$ The minimum, and maximum per-unit transformer tap-ratio values at branch i-j

μ The mean value of the probabilistic distribution function

σ The standard deviation value of the probabilistic distribution function

P_{best} The best location of each particle in PSO algorithm

G_{best} The best location of Pbest

$\overline{A}_1$ The average effect of level 1 of factor A on performance indicators

$\overline{A}_2$ The average effect of level 2 of factor A on performance indicators

$\overline{B}_1$ The average effect of level 1 of factor B on performance indicators

$\overline{B}_2$ The average effect of level 2 of factor B on performance indicators

$\overline{C}_1$ The average effect of level 1 of factor C on performance indicators

$\overline{C}_2$ The average effect of level 2 of factor C on performance indicators

ΔA The main effect of factor A on performance indicators

ΔB The main effect of factor B on performance indicators

ΔC The main effect of factor C on performance indicators

1. INTRODUCTION

Security and economy are two of the most critical issues in power system control, and operation. The security of the system refers to its ability to survive imminent disturbances (contingencies), without interruption in customer service [1]. Also, the economy of the system refers to optimizing the variable costs of operating the system. In this context, the SCOPF is another extended version of the OPF to model the security constraints from the operation of the power system by considering a set of postulated contingencies [2]. However, some references such as [3] have mainly focused on the great importance of voltage stability limits in modeling the SCOPF problem in the operation of competitive electricity markets, and have essentially evaluated and simulated the problem in terms of the voltage constraints.

This problem is a non-convex, nonlinear, and large-scale mixed-integer non-linear (MINL) optimization problem, including both discrete, and continuous variables [4], which is mainly handled through preventive control (PC), or corrective control (CC).

In recent years, the increasing growth of electricity consumption and, consequently, the extreme increase in the environmental pollution caused by the emission of toxic gases in thermal power plants, have increased the use of renewable energies, as an effective solution in this field. The application of the wind and solar resources, because of their numerous benefits, is at the center of the attention of power system planners, and operators.

Wind energy has many advantages over other forms of energy, such as no need for fuel, free access to it, no need for water, the low land area required for installation, and no environmental pollution tax. In recent years, with the increased use of renewable energy sources such as wind energy, the presence of uncertainties in the power system has become more significant. Deterministic approaches are not able to handle the uncertain OPF. A review of the literature indicates that there are some studies regarding the uncertain OPF, which are mainly classified as probabilistic approaches [5], stochastic methods [6], and robust techniques [7]. These techniques can also be categorized using techniques for the realization of the uncertainty of random variables, i.e., scenario-based approach [8] and interval optimization [9]. However, modeling different uncertainties, by using the conditional value-at-risk (CVaR) as a risk measurement tool, is of great importance [10].

Probabilistic optimal power flow (POPF), by considering the security constraints in the presence of the uncertain load and generation, has become an increasingly important topic in maintaining the reliability of the power system [11]. This concept, which is known as the uncertain-security constrained optimal power flow (USCOPF), deals with the SCOPF in the presence of different uncertainties in the power system. Although various techniques have been suggested to solve this complex and nonlinear problem, one of the main challenges is to find a solution that remains resistant to uncertainty, a topic which is known as the robust security-constrained (RSC) OPF [12].

The literature review shows that there are several studies conducted on SCOPF. A combination of preventive and correction control actions has been presented for the secured optimal power flow (SOPF) in [13].

In Ref. [12], the SCOPF problem has been solved using a parallel distributed memory structure exploiting framework, BELTISTOS-SC, to accelerate the SCOPF solutions over other techniques, and based on applying a structure-exploiting interior-point (IP) method.

In [14], PC actions have been outlined in the DCSOPF problem by using the BD. In [15], a contingency partitioning approach based on the differential evolution algorithm (DEA) has been proposed for the SCOPF problem, in both preventive and corrective stages, and the simulation results on the IEEE 118-bus system have been reported.

In [16], the SCOPF has been investigated in mixed AC/DC grids considering AC/DC and DC/DC converters, and based on no-linear models. Also, the case study results on the IEEE 14-bus system are detailed by the authors. Cao et al. [17] have analyzed the impacts of distributed energy storage systems on improving the power system reliability using an improved corrective SCOPF. They modeled the current state of charge (SOC) and the energy capacity in the suggested approach.

In [18], as the supplementary discussion of [13], the authors analyzed the impacts of hybrid energy storage systems (HESS) on keeping the power network stable, by applying enhanced corrective SCOPF. They considered the CC actions in the proposed model, which was solved by using improved Benders decomposition (BD) technique.

Reference [19], as the supplementary work for the previous research described in [14], has studied the SCOPF problem based on the scenario-decomposition approach in multiple microgrids based on some CC actions under uncertain generation and load demand. The authors proposed an incentive-based method to encourage the microgrids to cooperate with the main power grid for post-contingency recovery.

Reference [20], has presented a robust decomposition-based method for the generation dispatch of power systems, while sustaining the transient stability based on stochastic modeling of wind power generation. The proposed problem was modeled as an augmented OPF considering differential-algebraic equations and uncertain variables, and by converting the stability constraints to approximately-equivalent algebraic formulations.

The SCOPF problems were solved by applying a Hybrid Canonical DE-Particle Swarm Optimization (hC-DEEPSO) in [21]. The proposed algorithm was investigated on the IEEE 57-, 118-, and 300-bus standard systems.

An optimization technique based on the cross-entropy (CE) method has been proposed to solve the stochastic SCOPF problem in [22]. The solution quality was demonstrated by applying the suggested approach to the IEEE 57, and 300 buses, as the test cases.

Solving the SCOPF problem, in the presence of conflicting contingencies, has been addressed by applying a relaxing technique, either the set of control variables or operational constraints, in [23]. The SCOPF problem was solved by considering the dynamic thermal rating (DTR) of transmission lines, in a multi-objective manner, by applying an enhanced version of the goal attainment technique [24].

To solve the SCOPF, a new fuzzy adaptive artificial physics optimization (FAAPO) algorithm was adopted in ref. [25], by considering wind and thermal power generators. The proposed method was simulated on the IEEE 30-bus and Indian 75-bus systems.

In [26], to reduce the dimension of the SCOPF problem, each contingency was partitioned into three regions of internal, external, and boundary. For the internal region, the relevant variables would be more affected by the contingency. The external region was the rest of the network, and the final region included some buses at the external region connecting this region to an internal one. The SCOPF equations were linearized, and the selected variables and equations in the external region were omitted. Furthermore, the case study simulations on the IEEE 39 and 118 buses were detailed.

Yang et al. [27] addressed a parallel method for solving the interval DC SCOPF by considering demand uncertainties, and by applying the interval optimization method. The mentioned problem was transformed into two deterministic nonlinear programming problems and solved by the alternating direction method of multipliers (ADMM).

The SCOPF by considering critical contingencies, has been investigated in [28] which aimed to minimize the total generation cost by applying an interior-point (IP) algorithm. The linear sensitivity factors (LSFs) by using the Z-bus were modeled in the proposed technique. Two contingency filtering methods to accelerate the iterative solution of the SCOPF, based on considering preventive actions were demonstrated in [29].

Vaahedi et al. [30] proposed an approach for SCOPF and VAr planning under normal and post-contingency conditions considering the static for the security observing voltage profile and flow constraints. They extended the proposed technique to model dynamic security. An algorithm for solving the SCOPF problem by applying evolutionary programming (EP) has been proposed in [31].

The corrective SCOPF problem was solved by using an iterative approach comprising four modules and by applying BD [32]. The mentioned modules were considered only as a subset of potentially binding contingencies among the postulated contingencies, a steady-state security condition, a contingency filtering technique, and an OPF variant to check the post-contingency state feasibility.

In [33], a global optimization algorithm based on the Lagrangian duality has been proposed to solve the SCOPF problem by applying two decomposition algorithms based on Benders cut and the alternating direction method of multipliers.

The SCOPF problem in a large-scale power system was solved by applying an iterative algorithm, based on the combination of a contingency filtering scheme, and a network compression method in ref. [34]. The proposed method was simulated on a national grid with 2,563 buses and 1,297 contingencies, and the European transmission network with 9,241 buses and 12,000 contingencies.

The ant colony optimization (ACO) and modified bacteria foraging algorithm (MBFA) were applied to the SCOPF in the presence of wind power and incorporated with the thermal power plants, to minimize the operating cost, maintain a voltage secure operation, and minimize the system loss [35].

A corrective SCOPF problem based on sparse optimization techniques considering the DC power flow (DCPF) constraints, aimed to produce a generation schedule that had a minimal number of post-contingency corrections, and the minimum amount of total MW rescheduled was proposed by Phan et al. [36].

A flexible SCOPF, utilizing power router control in the post-contingency timeframe, and considering the FACTS-based power routers was proposed in [37]. Moreover, Jahan and Amjady [38] proposed a bi-level optimization approach to solve the SCOPF problem in an AC network, considering the prohibited operating zone, multi-fuel option, and valve loading effect constraints.

The Lagrangian relaxation, and BD techniques were applied to the corrective risk-based SCOPF problem in [39]. Both circuit and system risks were considered in this study. A multi-agent-based, fully distributed DC SCOPF approach in the presence of DGs based on solving the first-order optimality conditions through an iterative process was addressed in [40].

In ref. [41], a robust DC-OPF technique based on applying Taguchi's orthogonal array has been proposed, in which the probability of load and renewable energies have been mentioned. The security constraints, or operation contingencies, are not mentioned in the suggested approach. Also, the simulation results of the suggested method on some cases up to 2,736 buses have been addressed.

In [42], a framework to capture previously intractable optimization constraints and transform them into an MILP, by using the neural networks in a deterministic power system, was presented. The feasible space of optimization problems characterized by different constraints was encoded to a neural network. The ACOPF was used, and n-1 security and small-signal stability were mentioned in the suggested model.

Velay et al. [43] introduced a fully distributed method to solve the DC-SCOPF by considering the automatic primary frequency response of generators after an incident via the alternating direction method of multipliers (ADMM).

As the literature review suggests, only a few studies, such as [14, 19, 20] have addressed the RSCOPF problem. Also, only a few studies have investigated the impacts of different uncertainties such as uncertain load and wind power plant generation in the problem. References [14, 19, 20, 25] are good examples for this category.

One of the objectives of the present study is to investigate the impacts of uncertain parameters based on the proposed method and to determine the effect of different contingencies of line and unit outages on the optimal operation cost (i.e., OPF) for the secure operation of the power system. Based on this, it is possible to perform an appropriate PC by classifying the effect of each contingency.

The main novelties of this work, compared to other works in this field (especially reference [14]), are as follows:

- Modeling the SCOPF by using the AC power flow (ACPF), which is solved by applying the PSO algorithm due to the fast convergence, for the first time for this type of problem
- Modeling the security constraints, directly and completely, as one of the constraints in the optimization problem, without any simplifications
- Introducing the most critical generation units and transmission lines, whose loss imposes the highest operating costs on the network, based on applying the n-1 and n-2 security criteria
- Modeling the wind power generation and demand load uncertainties as a package by using the TOAT method in order to decrease the run-time for solving the RSCSOPF problem.

The remainder of this paper is organized as follows: The second section details the objective function and the relevant constraints regarding the SCOPF problem. In the third section, the TOAT is investigated. The suggested method's performance is addressed in the fourth section by detailed case study simulations on the IEEE 14-bus system. Finally, the last section presents the main conclusions.

2. FORMULATION OF THE SCOPF

The purpose of OPF is to determine the optimal amount of generations that minimize the cost of operation, by considering the relevant constraints and security limits.

A. Objective function

The objective function is the cost of fuel for all generation units as:

$$\min \sum_{i \in n_g} \left(a_i P_{Gi}^2 + b_i P_{Gi} + c_i \right) \tag{1}$$

in which, P_{Gi} is the output power of unit i. Moreover, a_i, b_i ,and c_i are the cost coefficients for the i-th unit.

B. The constraints

The most important constraints in the OPF problem are presented as follows:

b1) Generation and demand load equality constraint The most critical constraint in the power system is the balance between generation and load, as expressed in (2):

$$P = P_G - P_{Load} + P_{\text{Res}} \tag{2}$$

where, P is the bus injection power vector, P_G is the vector of the generation power, P_{Load} is the demand load vector, and P_{Res} is the power generation vector by wind power plants. The probabilistic form of Equation (2) is as follows:

$$\tilde{P} = P_G - \tilde{P}_{Load} + \tilde{P}_{\text{Res}} \tag{3}$$

where, $\tilde{P}$, $\tilde{P}_{Load}$, and $\tilde{P}_{Res}$ denote the probabilistic bus injection power vector, the probabilistic demand load vector, and the vector of probabilistic power generation by wind power plants, respectively.

b2) ACPF model The most crucial subject in the real-power systems is the ACPF model. Here, without simplification, the ACPF model is detailed as follows:

$$\begin{aligned} P_i &= |V_i| \sum_{j=1}^{n} \left|V_j\right| \left(G_{ij} \cos \varphi_{ij} + B_{ij} \sin \varphi_{ij} \right) \\ Q_i &= |V_i| \sum_{j=1}^{n} \left|V_j\right| \left(G_{ij} \cos \varphi_{ij} - B_{ij} \sin \varphi_{ij} \right) \end{aligned} \tag{4}$$

where, P_i represents the injection power for bus i, $|V_i|$ denotes the voltage magnitude of bus i, G_{ij}, and B_{ij} are the conductance and susceptance value for line L, connected between buses i and j, and φ_{ij} indicates the phase angle difference between buses i, and j.

$$P_L = |V_i|\,|V_i| \left(G_{ij} \cos \varphi_{ij} + B_{ij} \sin \varphi_{ij} \right) - n_{ij} G_{ij} \,|V_i|^2 \tag{5}$$

where P_L is the power flow of line L between buses i, and j and n_{ij} is the per-unit transformer tap-ratio located at branch i-j.

Also, the main governing constraints of the ACPF are as:

$$\begin{aligned} &\underline{P_G} \le P_G \le \overline{P_G}, \quad \underline{Q_G} \le Q_G \le \overline{Q_G} \\ &|\underline{V_i}| \le |V_i| \le \overline{|V_i|} \\ &\underline{n_{ij}} \le n_{ij} \le \overline{n_{ij}} \end{aligned} \tag{6}$$

The generated active and reactive powers (P_G, Q_G) should be limited within the relevant minimum ($\underline{P_G}$, $\underline{Q_G}$) and maximum ($\overline{P}_G$, $\overline{Q}_G$) values. The voltage magnitude for each bus ($|V_i|$) is limited by the minimum ($\left|\underline{V_i}\right|$) and maximum ($|\overline{V_i}|$) values. Also, the transformer tap-ratio (n_{ij}) is limited in the range of the minimum ($\underline{n_{ij}}$) and maximum ($\overline{n}_{ij}$) values.

b3) System security constraints There may be many events in a power system, a large number of which, or at least the most probable ones, should be studied and analyzed such that the

relevant overload conditions are mentioned by operators before the occurrence of contingencies. The use of the generation shift factor (GSF) method is one of the effective techniques in this regard [44]. These coefficients show a relative change in the transmission line power due to changes in the injectable power and are approximately calculated by using DCPF. Generally, these coefficients are calculated as follows:

$$h_{Li} = \frac{\Delta P_{line}}{\Delta P_i} \tag{7}$$

in which ΔP_{line}, is the change in the power flow on line L, due to the change in the injection power of unit i. The GSFs can be expressed in a general form by using the H-matrix, as follows:

$$P_{line} = HP \tag{8}$$

P_{Line} is the power matrix of the lines. The power flow on all the lines should be within the allowable range, as follows:

$$\underline{P}_{line} \le P_{line} \le \overline{P}_{line} \tag{9}$$

$$\underline{P}_{line} = -\overline{P}_{line} \tag{10}$$

By placing (8) in (9), Equation (11) is obtained, as follows:

$$-\overline{P}_{line} \le HP \le \overline{P}_{line} \tag{11}$$

By placing Equation (3) in (11):

$$\begin{aligned} &-\overline{P_{\text{Line}}} - H\tilde{P}_{\text{Res}} + H\tilde{P}_{\text{Load}} \le HP_G \\ &\le \overline{P_{\text{Line}}} - H\tilde{P}_{\text{Res}} + H\tilde{P}_{\text{Load}} \end{aligned} \tag{12}$$

By selecting the non-zero entries of $\tilde{P}_{\text{Res}}$, $\tilde{P}_{\text{Load}}$, and P_G, in (12), the H matrix by multiplying each of them is converted into H_{Res}, H_{Load}, and H_G, respectively.

Equation (12) can be re-written as (13), which is known as the system security constraint.

$$\begin{aligned} -\overline{P_{\text{Line}}} - H_{\text{Res}}\tilde{P}_{\text{Res}} + H_{\text{Load}}\tilde{P}_{\text{Load}} \le H_G P_G \\ \le \overline{P_{\text{Line}}} - H_{\text{Res}}\tilde{P}_{\text{Res}} + H_{\text{Load}}\tilde{P}_{\text{Load}} \end{aligned} \tag{13}$$

3. THE TOAT

A powerful method to convert the uncertain values into deterministic ones is the TOAT, which is based on orthogonal arrays. Using these orthogonal arrays, it is possible to select the minimum number of uncertainties with minimal experiments. Generally, the $L_e y^u$ orthogonal array describes the arrangements of e experiments with u uncertain parameters, in which each parameter has y levels [45]. The smallest orthogonal array is $L_4 2^3$, which makes it possible to perform four experiments with three double-level factors, such as those given in Table 1. In the TOAT, the word *factor* refers to a random variable, and the word *level* indicates the amount taken up from the probability distribution.

Taguchi has presented different orthogonal arrays for different numbers of factors and levels. The Taguchi orthogonal arrays for two-level factors are $L_{32}2^{31}$, $L_{16}2^{15}$, $L_{12}2^{11}$, $L_8 2^7$, and $L_4 2^3$. For example, if 25 factors are mentioned in the problem, then the $L_{32}2^{31}$ should be selected, and the remaining six columns should be ignored. TOAT converts the uncertain parameters into certain ones in three steps, as follows:

Step one: Determining the number of levels for each factor

Table 1. The Taguchi orthogonal array $L_4 2^3$ [22]

Experiment	Level for each factor		
	Factor A	Factor B	Factor C
1	1	1	1
2	1	2	2
3	2	1	2
4	2	2	1

The first step in using the TOAT to solve a probabilistic power flow problem is to determine the number of levels of each factor. TOAT with two-level factors requires the least amount of calculations, while using three-level factors requires a long computing time. For the same reason, here, the TOAT with two-level factors is applied.

Step two: Determining the levels of factors

The next step in the TOAT is to determine the levels of factors. It is always possible to set up two levels of a random variable by using a probabilistic Gaussian distribution function. Here, the load demand is modeled as the Gaussian probabilistic distribution function, and the two levels of the demand load are assumed as $\mu + \sigma$ (as level one) and $\mu - \sigma$ (as level two). The μ, and σ describe the mean and standard deviation values of the Gaussian probabilistic distribution function, in that order. The wind power generation by a wind plant is modeled using the Weibull distribution function, and two-level experiments are assumed to be as $\mu + \sigma$, and $\mu - \sigma$.

Step 3: Optimal experiment design

In the last step, an approximate solution to the probabilistic power flow with the best performance index is obtained. It should be mentioned that the term optimal does not imply the optimization methods. An optimal experiment is achieved by using the following three steps:

1) In the first step, a performance index is defined for each experiment, as follows:

$$Y_j = \sum_{L=1}^{NL} \left| f_{jL} - f_l^* \right|, \qquad j = 1, 2, 3, ..., N \tag{14}$$

where NL denotes the number of branches, N indicates the number of experiments, f_{jL} represents the power flow on line L obtained from the power flow calculations regarding experiment j, and f_l^* indicates the nominal power flow on line L.

2) In the second step, the average effects of the levels of factors on performance indicators are calculated. For example, in Table 1, including four experiments, the average effects of the levels of factors are defined as the set of Equations (15), in which the average effects of different levels of factors on the performance indicators are defined as:

$$\begin{aligned} \bar{A}_1 &= (Y_1 + Y_2)/2, \quad \bar{A}_2 = (Y_3 + Y_4)/2 \\ \bar{B}_1 &= (Y_2 + Y_4)/2, \quad \bar{B}_2 = (Y_1 + Y_3)/2 \\ \bar{C}_1 &= (Y_2 + Y_3)/2, \quad \bar{C}_2 = (Y_1 + Y_4)/2 \end{aligned} \tag{15}$$

3) In the third step, the main effect of each factor on the performance indicators is defined and is obtained by subtracting the effect of the second level from the effect of the first one:

$$\begin{aligned} &\Delta A = \bar{A}_2 - \bar{A}_1, \quad \Delta B = \bar{B}_2 - \bar{B}_1, \\ &\Delta C = \bar{C}_2 - \bar{C}_1 \end{aligned} \tag{16}$$

If the main effect of a factor is positive, the second level of this factor is considered in the optimal experiments. When it is negative, the first level of this factor is considered in the optimal experiment.

4. SOLUTION METHOD

In this section, the solution algorithms and the methods which are used for ACOPF, and handling the RSCOPF problems are detailed. The ACOPF is solved by PSO, and the other problem is run by using a mathematical-iterative based approach. Some brief explanations on these issues are addressed below.

A. ACOPF by PSO

The ACOPF is a non-linear, and complex problem and is usually solved by applying some heuristic algorithms. Here, the PSO is employed to solve this problem. In the PSO, each particle is an m-dimensional vector, where m is the number of optimization parameters. Each particle has five properties: position, position-corresponding to the objective function, velocity, best-experienced personal, and global positions. The details can be found in [46]. One of the most challenging issues regarding the application of heuristic algorithms is setting the algorithm parameters. As a general principle, tuning the parameters of heuristic algorithms is a compromise between the run-time and the accuracy of the solutions, and is performed by using a trial-and-error procedure. As the number of iterations grows, better answers are obtained over a longer run-time. However, this trend will be reversed as the number of iterations decreases. This is completely true for selecting the swarm size. Here, the procedure is implemented for different setting parameters in various cases, and it is concluded that it will be possible to choose an acceptable and logical compromise between run-time and accuracy by selecting the setting parameter as: the maximum number of iterations = 100, population size (swarm size) = 20; inertia weight = 1, inertia weight damping ratio = 0.99, personal learning coefficient = 2, and global learning coefficient = 2.

Fig. 1 illustrates a simple flowchart for PSO, which is used for ACOPF.

B. The solution method of the RSCOPF problem

Fig. 2 depicts the flowchart of solving the RSCOPF problem for *n-1* and *n-2* line, and unit contingencies, separately. As an important note, the RSCOPF is run with the number of lines, in the case of the *n-1* contingency. Also, in the case of the *n-2* contingency, the problem is run for a hundred scenarios. Each scenario simultaneously defines the outage of two lines. These scenarios are randomly generated according to the Gaussian probabilistic distribution function. Furthermore, the RSCOPF is run with the number of generation units (except for the reference one) in the case of the *n-1* contingency. The *n-2* contingency is run only for the outage of units #6 and #8.

5. CASE-STUDY SIMULATION RESULTS

The proposed algorithm is implemented using the MATLAB software on the IEEE 14-bus system, which contains 11 demand loads and five power generation units. Two wind power plants are located in buses 2 and 3. Given that there are 13 random variables (11 demand loads and two wind power plants), the Taguchi orthogonal array of $L_{16}2^{15}$, which includes 16 experiments, is used. Levels one and two for wind power plants are considered to be equal to zero and 40 MW, respectively. Also,

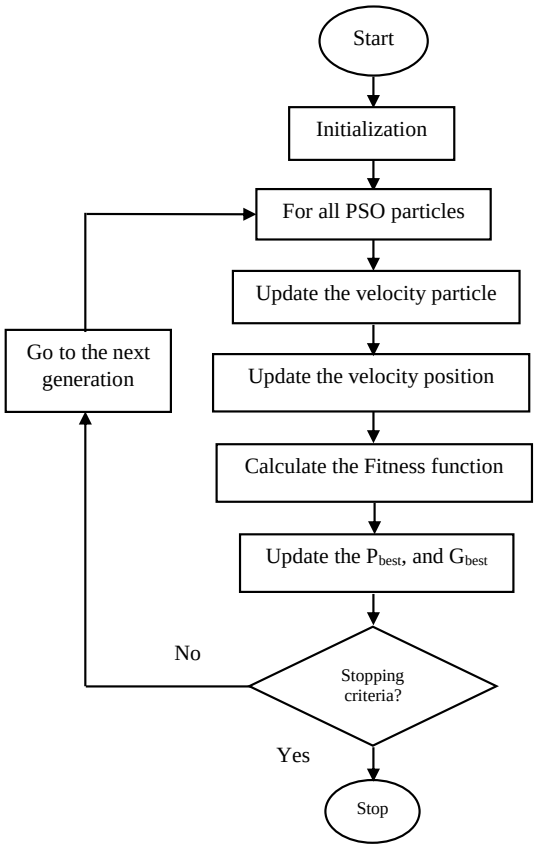

Fig. 1. A simple flowchart of the PSO.

these levels for demand loads are supposed to be $\mu + \sigma$ and $\mu - \sigma$,respectively. The standard deviation is considered to be 15% of the mean value. Here, the mean value for each load is selected as the standard load value based on the IEEE 14-bus data [47]. Using the TOAT, the uncertainties are converted into deterministic ones, and then the optimization problem considering the security constraints obtained by the Taguchi result is investigated. Different results are presented below. To solve the optimization problem, the PSO algorithm is applied due to its advantages over the other optimization methods. To handle the constraints, all of them are checked at each step of the algorithm implementation. In the case of the violation of any of the modeled constraints, the evaluation function or cost function is selected equal to a very large number. Thus, in selecting the best solution in each stage as the local best position or global best position, the relevant cost function will be omitted.

A. Deterministic power flow (DPF)

When the uncertainties are converted into deterministic parameters by the Taguchi model, the results are obtained in the form of deterministic values, as shown in Figs. 3-7. The base of power is 100 MW, the maximum number of iterations is 100, and the accuracy for checking the ACLF convergence is assumed to be equal to 0.0001.

The performance index of the deterministic power flow is 1.4579, which exceeds the performance indicators derived from the 16 Taguchi experiments by TOAT.

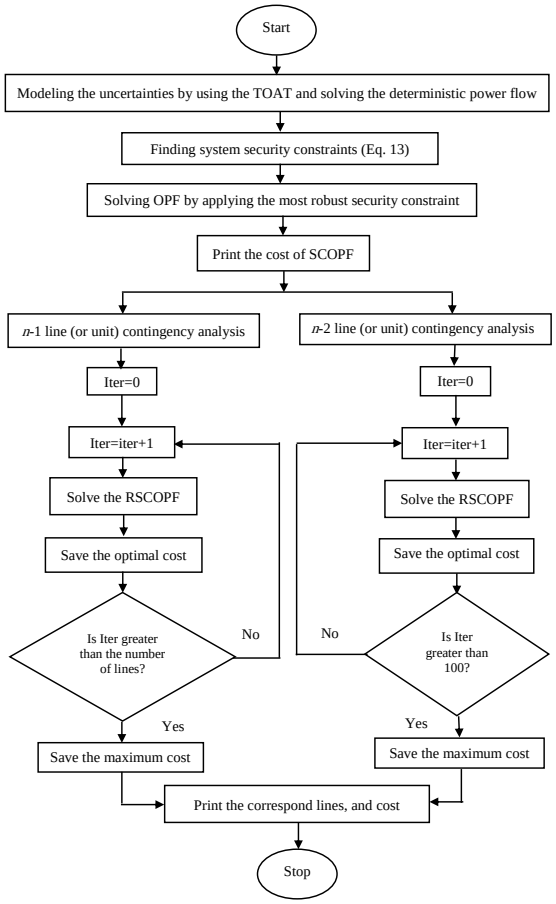

Fig. 2. The proposed flowchart for the RSCOPF problem.

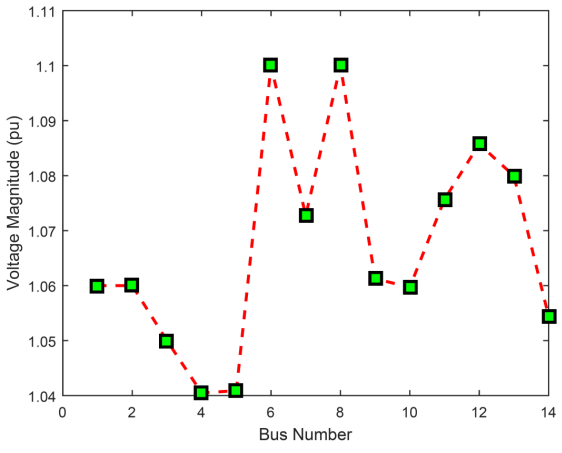

Fig. 3. The voltage magnitudes for the deterministic power flow.

B. RSCOPF

The results obtained by applying the deterministic results derived from the Taguchi model are called a robust OPF. These results with and without the relevant constraints are presented in Tables 2 and 3, respectively. In addition, the convergence curve of the PSO algorithm for the RSCOPF is depicted in Fig. 8.

By comparing Tables 2 and 3, it is observed that the optimal operation cost while neglecting the constraints is less than the optimal operation cost while taking into account the constraints. When there is no constraint, there is a more satisfactory solution for the problem, and the solution may be smaller due to the cost reduction.

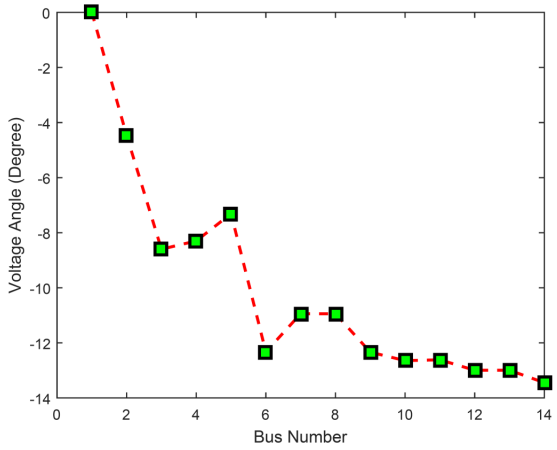

Fig. 4. The voltage angles for the deterministic power flow.

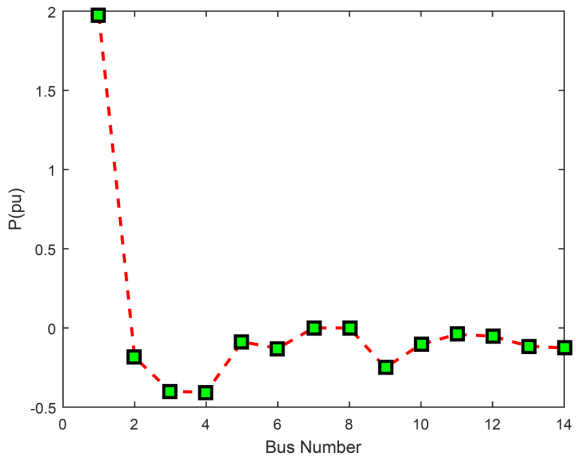

Fig. 5. The injected power for the deterministic power flow.

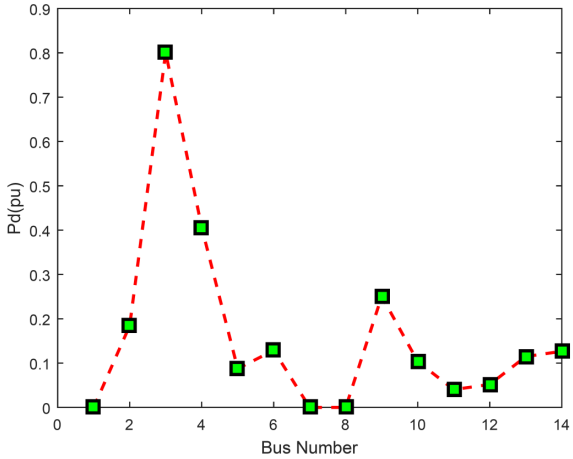

Fig. 6. The active power for demand loads in the deterministic power flow.

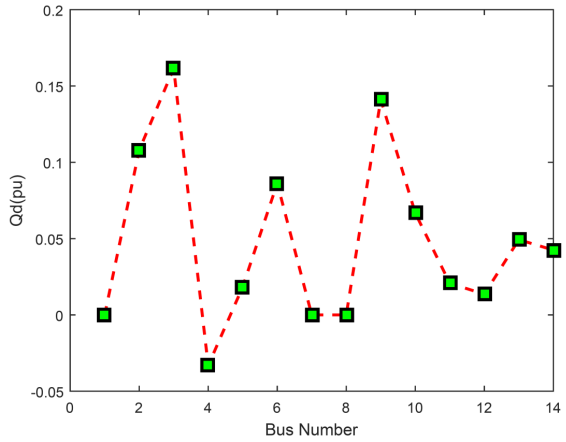

Fig. 7. The reactive power for demand loads in the deterministic power flow.

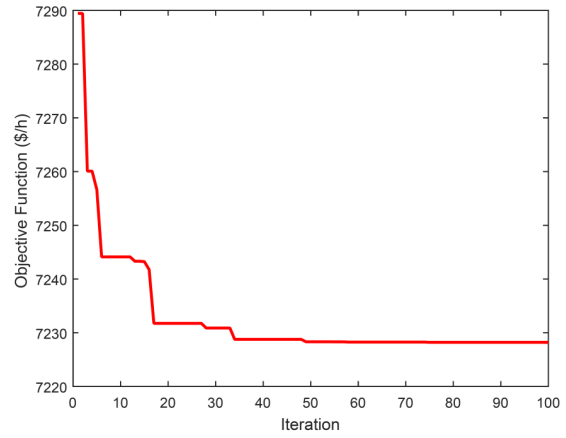

Fig. 8. The convergence curve of the PSO algorithm for RSCOPF.

C. Results of applying 16 Taguchi experiments on OPF by TOAT

The results of 16 Taguchi experiments on the OPF problem are given in Table 4.

By comparing the RSCOPF with the costs of the 16 Taguchi experiment, it is found that the cost of the RSCOPF is smaller than the other costs. The main reason for this is that it has the most robust security constraint, which is very likely to be violated.

D. The result of the *n-1* contingency security analysis for single-line outage

To check the *n-1* contingency security, the RSCOPF is run by considering a single-line outage in each step. The results are presented in Table 5, in which the costs are ranked in the ascending order of cost.

Evidently, the most critical lines whose outage will result in the highest cost increase are at first the line number one (connected between buses 1 and 2), and then line number two (connected between buses 1 and 5). Since these lines are both connected to bus 1, bus 1 or the reference bus is the most critical. It is necessary to prevent the outage of the lines connected to it as far as possible.

Table 2. RSCOPF results

Generated Powers (pu)			Cost ($/hr)
PG1	PG2	PG3	
1.15	0.385	0.3952	7,227.27

Table 3. Robust OPF while neglecting the constraints

Generated Powers (pu)			Cost ($/hr)
PG1	PG2	PG3	
1.55	0.077	0.311	6,934.62

Table 4. Sixteen Taguchi experiments on OPF

Experiment No.	Generated Powers (pu)			Cost ($/hr)
	PG1	PG2	PG3	
1	1.09	0.778	0.382	7,414
2	1.095	1	0.395	8,405
3	1.454	1	0.399	12,976
4	1.515	1	0.399	13,653
5	1.127	0.46	0.396	7,472
6	1.128	0.638	0.396	8,200
7	1.082	0.978	0.397	9,485
8	1.082	0.978	0.4	9,531
9	1.156	0.635	0.398	8,278
10	1.152	0.687	0.399	8,492
11	1.072	0.852	0.399	9,937
12	1.091	0.896	0.399	10,209
13	1.2	0.288	0.211	7,432
14	1.197	0.306	0.26	7,695
15	1.243	0.236	0.367	7,990
16	1.244	0.284	0.394	8,295

E. The result of the *n-2* contingency security analysis for double-line outages

To check the *n-2* contingency security analysis, two lines are removed from the service at the same time; subsequently. The RSCOPF is run, accordingly. To do this, 100 random scenarios describing the simultaneous outage of two lines, are considered. The results are ranked in the ascending order of cost. As a result, 20 random scenarios with the highest operating costs are shown in Table 6. The nature of the line outage uncertainty is completely different from the wind generation or load demand patterns. The generation and load can be modeled as the Gaussian probabilistic distribution functions, whereas the line outage uncertainty cannot be modeled in this way. Therefore, to handle the line outages' uncertainty, the random scenarios are employed.

As can be seen, the most critical line whose outage will result in the highest cost increase is the line number one (connected between buses 1 and 2). The preventive action controls should be performed such that this line is not removed.

Table 5. The *n-1* contingency security analysis for the single-line outage

No. of the faulted line (From bus- To bus)	Cost ($/hr)
5 (2-5)	7,150.99
4 (2-4)	7,168.57
3 (2-3)	7,205.93
9 (4-9)	7,227.66
8 (4-7)	7,228.36
16 (9-10)	7,228.43
19 (12-13)	7,228.66
15 (7-9)	7,229.59
10 (5-6)	7,229.73
18 (10-11)	7,231.37
17 (9-14)	7,232.22
12 (6-12)	7,233.53
20 (13-14)	7,233.87
11 (6-11)	7,239.25
14 (7-8)	7,240.07
13 (6-13)	7,252.53
6 (3-4)	7,265
7 (4-5)	7,398.91
2 (1-5)	7,617.90
1 (1-2)	9,080.79

Table 6. The *n-2* contingency security analysis for double-line outages

No. of faulted lines (From bus- To bus)		Cost ($/hr)
2 (1-5)	19 (12-13)	7,616.75
2 (1-5)	18 (10-11)	7,617.59
2 (1-5)	20 (13-14)	7,619.55
2 (1-5)	12 (6-12)	7,620.46
2 (1-5)	15 (7-9)	7,637.56
13 (6-13)	2 (1-5)	7,639.67
3 (2-3)	2 (1-5)	7,653.37
19 (12-13)	13 (6-13)	7,685.78
13 (6-13)	17 (9-14)	7,722.71
12 (6-12)	13 (6-13)	8,244.37
7 (4-5)	3 (2-3)	9,054.87
1 (1-2)	17 (9-14)	9,078.94
4 (2-4)	1 (1-2)	9,081.28
1 (1-2)	6 (3-4)	9,096.28
1 (1-2)	3 (2-3)	9,104.55
18 (10-11)	1 (1-2)	9,637.04
20 (13-14)	1 (1-2)	9,709.03
1 (1-2)	11 (6-11)	10,001.11
7 (4-5)	1 (1-2)	11,155.54
1 (1-2)	10 (5-6)	11,455.35

F. The result of the *n-1* contingency security analysis for single-unit outage

To check the *n-1* contingency security, the RSCOPF is run by considering a single-unit outage in each step. The results are given in Table 7, in which the costs are ranked in the ascending order of cost.

The most critical generation unit whose outage will result in the highest cost increase is generation unit #6. It is essential to prevent the outage of this unit as far as possible.

G. The result of the *n-2* contingency security analysis for two-unit outages

To check the *n-2* contingency security analysis, two generation units (except for reference one) are removed from the service at the same time; then, the RSCOPF is run accordingly. The result is addressed in Table 8.

The cost function in this case is increased at least to $\sim$ 40% more than the highest cost function of the *n-1* contingency security analysis for the single-line outage. This means that such a situation should be prevented in the system as far as possible.

H. Discussion

Despite the multiplicity of methods proposed for this purpose, it is not possible to numerically compare the results due to the differences in the nature of the proposed methods. However, to validate the results, the findings of different cases by the proposed method are compared with each other in Table 9.

By adding the constraints to the problem, the cost function will be increased by 5%. Also, considering the contingency security analysis for line outages reveals that the cost function for the *n-2* case will be increased by at least 6.5% to 26%. Furthermore,

Table 7. The *n-1* contingency security analysis for single-unit outage

Unit outage	P_{G1} (pu)	P_{G6} (pu)	P_{G8} (pu)	Cost ($/hr)
# 6	1.5472	0	0.4	10,075.18
# 8	1.1425	0.8	0	7,301.98

Table 8. The *n-2* contingency security analysis for two-unit outages

Unit outage	P_{G1} (pu)	P_{G6} (pu)	P_{G8} (pu)	Cost ($/hr)
# 6 and # 8	1.9775	0	0	13,955.063

mentioning the contingency security analysis for unit outages demonstrates that the cost function for the *n-2* case will be increased by at least 40%. The results indicate the accuracy of the proposed method.

The main advantages of the TOAT are its easy application, high speed of uncertain problem solving, and acceptable accuracy when compared to the other probabilistic methods, especially the scenario generation techniques, by limiting the number of solving the problem. Besides, the required run-time for all of the other issues such as *n-1* and *n-2* contingency analysis is the same for the proposed methods in the field of RSCOPF. Also, the application of heuristic methods, such as PSO, assists in finding more accurate and reliable solutions which cannot be handled by the mathematical-based solutions in most cases. Of course, it is noteworthy that the online application of this method requires advanced computational methods such as parallel processing

Table 9. Comparative analysis for different cases

Item	Description	Cost ($/hr)
1	ROPF without constraints	6,934.62
	RSCOPF	7,227.27
2	n-1 contingency security analysis for single line outage	Min: 7,150.99, Max: 9,080.79
	n-2 contingency security analysis for double line outages	Min: 7,616.75, Max: 11,455.35
3	n-1 contingency security analysis for single unit outage	Min: 7,301.9787, Max: 10,075.1815
	n-2 contingency security analysis for two unit outages	13,955.06

and the use of high-speed processing tools.

6. CONCLUSION

The application of the TOAT for analyzing load and wind power uncertainties was discussed. Since the two-level Taguchi method requires the least amount of OPF calculations compared to the three-level Taguchi method, only two levels of each factor were considered in the analysis. By using the TOAT, different uncertainties were changed into traditional deterministic values, and solving the relevant OPF problem led to the best performance index. Also, the RSCOPF problem was analyzed completely by applying the ACPF and by using the PSO algorithm. Finally, based on (*n-1*), and (*n-2*) contingency security analysis, some useful results were addressed. The TOAT is an economical, quick, simple, and feasible technique for designing high-quality processes with less variance for experiments in defining the proper control factors to achieve optimum results. The main disadvantage of the TOAT is that the results are only relative and do not exactly show what parameter has the highest effect on the performance characteristic value. Some open issues which are currently the subject of further research include solving the RSCOPF problem by applying the information gap decision theory (IGDT), and robust scenario-generation technique. Moreover, modeling the outage probability of the lines can be an interesting topic in this regard.

REFERENCES

1. K. Morison, L. Wang, and P. Kundur, "Power system security assessment," IEEE power and energy magazine, vol. 2, no. 5, pp. 30-39, 2004.
2. H. Abdi, S. D. Beigvand, and M. La Scala, "A review of optimal power flow studies applied to smart grids and microgrids," Renewable and Sustainable Energy Reviews, vol. 71, pp. 742-766, 2017.
3. F. Milano, C. A. Cañizares, and A. J. Conejo, "Sensitivity-based security-constrained OPF market clearing model," IEEE Transactions on power systems, vol. 20, no. 4, pp. 2051-2060, 2005.
4. F. Capitanescu et al., "State-of-the-art, challenges, and future trends in security constrained optimal power flow," Electric Power Systems Research, vol. 81, no. 8, pp. 1731-1741, 2011.
5. M. Shukla and G. Radman, "Optimal power flow using probabilistic load model," in Proceedings of the Thirty-Seventh Southeastern Symposium on System Theory, 2005. SSST'05., 2005: IEEE, pp. 439-442.
6. T. Yong and R. Lasseter, "Stochastic optimal power flow: formulation and solution," in 2000 Power Engineering Society Summer Meeting (Cat. No. 00CH37134), 2000, vol. 1: IEEE, pp. 237-242.
7. T. Zheng, J. Zhao, E. Litvinov, and F. Zhao, "Robust optimization and its application to power system operation," in CIGRE, 2012.
8. A. Alabdulwahab, A. Abusorrah, X. Zhang, and M. Shahidehpour, "Coordination of interdependent natural gas and electricity infrastructures for firming the variability of wind energy in stochastic day-ahead scheduling," IEEE Transactions on Sustainable Energy, vol. 6, no. 2, pp. 606-615, 2015.
9. Z. Wang and F. L. Alvarado, "Interval arithmetic in power flow analysis," IEEE Transactions on Power Systems, vol. 7, no. 3, pp. 1341-1349, 1992.
10. M. Vahedipour-Dahraie, H. Rashidizadeh-Kermani, A. Anvari-Moghaddam, and J. M. Guerrero, "Stochastic Risk-Constrained Scheduling of Renewable-Powered Autonomous Microgrids with Demand Response Actions: Reliability and Economic Implications," IEEE Transactions on Industry Applications, 2019.
11. R. Zhang, Z. Y. Dong, Y. Xu, K. P. Wong, and M. Lai, "Hybrid computation of corrective security-constrained optimal power flow problems," IET Generation, Transmission & Distribution, vol. 8, no. 6, pp. 995-1006, 2014.
12. J. Kardoš, D. Kourounis, and O. Schenk, "Two-Level Parallel Augmented Schur Complement Interior-Point Algorithms for the Solution of Security Constrained Optimal Power Flow Problems," IEEE Transactions on Power Systems, 2019.
13. Y. Xu, Z. Y. Dong, R. Zhang, K. P. Wong, and M. Lai, "Solving preventive-corrective SCOPF by a hybrid computational strategy," IEEE Transactions on Power Systems, vol. 29, no. 3, pp. 1345-1355, 2013.
14. W. Zhang, Y. Xu, Z. Y. Dong, Y. Wang, and R. Zhang, "An efficient approach for robust SCOPF considering load and renewable power uncertainties," in 2016 Power Systems Computation Conference (PSCC), 2016: IEEE, pp. 1-7.
15. Y. Xu, H. Yang, R. Zhang, Z. Y. Dong, M. Lai, and K. P. Wong, "A contingency partitioning approach for preventive-corrective security-constrained optimal power flow computation," Electric Power Systems Research, vol. 132, pp. 132-140, 2016.
16. V. Saplamidis, R. Wiget, and G. Andersson, "Security constrained optimal power flow for mixed AC and multi-terminal HVDC grids," in 2015 IEEE Eindhoven PowerTech, 2015: IEEE, pp. 1-6.
17. J. Cao, W. Du, and H. Wang, "An improved corrective security constrained OPF with distributed energy storage," IEEE Transactions on Power Systems, vol. 31, no. 2, pp. 1537-1545, 2015.
18. J. Cao, Y. Liu, Y. Ge, H. Cai, and B. Zhou, "Enhanced corrective security constrained OPF with hybrid energy storage systems," in 2016 UKACC 11th International Conference on Control (CONTROL), 2016: IEEE, pp. 1-7.
19. W. Zhang, Y. Xu, Z. Dong, and K. P. Wong, "Robust security constrained-optimal power flow using multiple microgrids for corrective control of power systems under uncertainty," IEEE Transactions on Industrial Informatics, vol. 13, no. 4, pp. 1704-1713, 2016.
20. Y. Xu, M. Yin, Z. Y. Dong, R. Zhang, D. J. Hill, and Y. Zhang, "Robust dispatch of high wind power-penetrated power systems against transient instability," IEEE Transactions on Power Systems, vol. 33, no. 1, pp. 174-186, 2017.
21. C. G. Marcelino et al., "Solving security constrained optimal power flow problems: a hybrid evolutionary approach," Applied Intelligence, vol. 48, no. 10, pp. 3672-3690, 2018.
22. L. de Magalhães Carvalho, A. M. L. da Silva, and V. Miranda, "Security-Constrained Optimal Power Flow via Cross-Entropy Method," IEEE Transactions on Power Systems, vol. 33, no. 6, pp. 6621-6629, 2018.
23. F. Capitanescu, "Approaches to Obtain Usable Solutions for Infeasible Security-Constrained Optimal Power Flow Problems Due to Conflicting

Contingencies," in 2019 IEEE Milan PowerTech, 2019: IEEE, pp. 1-6.
24. S. Rahmani and N. Amjady, "Enhanced goal attainment method for solving multi-objective security-constrained optimal power flow considering dynamic thermal rating of lines," Applied Soft Computing, vol. 77, pp. 41-49, 2019.
25. K. Teeparthi and D. V. Kumar, "Security-constrained optimal power flow with wind and thermal power generators using fuzzy adaptive artificial physics optimization algorithm," Neural Computing and Applications, vol. 29, no. 3, pp. 855-871, 2018.
26. F. Karbalaei, H. Shahbazi, and M. Mahdavi, "A new method for solving preventive security-constrained optimal power flow based on linear network compression," International Journal of Electrical Power & Energy Systems, vol. 96, pp. 23-29, 2018.
27. L. Yang, C. Zhang, and J. Jian, "A parallel method for solving the DC security constrained optimal power flow with demand uncertainties," International Journal of Electrical Power & Energy Systems, vol. 102, pp. 171-178, 2018.
28. D. B. Rathod and R. A. Jain, "Comparative Analysis on Security-Constrained Optimal Power Flow Using Linear Sensitivity Factors-Based Contingency Screening," in Innovations in Infrastructure: Springer, 2019, pp. 139-147.
29. F. Capitanescu, M. Glavic, D. Ernst, and L. Wehenkel, "Contingency filtering techniques for preventive security-constrained optimal power flow," IEEE Transactions on Power Systems, vol. 22, no. 4, pp. 1690-1697, 2007.
30. E. Vaahedi, Y. Mansour, C. Fuchs, S. Granville, M. D. L. Latore, and H. Hamadanizadeh, "Dynamic security constrained optimal power flow/var planning," IEEE Transactions on Power Systems, vol. 16, no. 1, pp. 38-43, 2001.
31. P. Somasundaram, K. Kuppusamy, and R. K. Devi, "Evolutionary programming based security constrained optimal power flow," Electric Power Systems Research, vol. 72, no. 2, pp. 137-145, 2004.
32. F. Capitanescu and L. Wehenkel, "A new iterative approach to the corrective security-constrained optimal power flow problem," IEEE transactions on power systems, vol. 23, no. 4, pp. 1533-1541, 2008.
33. D. Phan and J. Kalagnanam, "Some efficient optimization methods for solving the security-constrained optimal power flow problem," IEEE Transactions on Power Systems, vol. 29, no. 2, pp. 863-872, 2013.
34. L. Platbrood, F. Capitanescu, C. Merckx, H. Crisciu, and L. Wehenkel, "A generic approach for solving nonlinear-discrete security-constrained optimal power flow problems in large-scale systems," IEEE Transactions on Power Systems, vol. 29, no. 3, pp. 1194-1203, 2013.
35. A. Panda and M. Tripathy, "Security constrained optimal power flow solution of wind-thermal generation system using modified bacteria foraging algorithm," Energy, vol. 93, pp. 816-827, 2015.
36. D. T. Phan and X. A. Sun, "Minimal impact corrective actions in security-constrained optimal power flow via sparsity regularization," IEEE Transactions on Power Systems, vol. 30, no. 4, pp. 1947-1956, 2014.
37. J. J. Thomas and S. Grijalva, "Flexible security-constrained optimal power flow," IEEE Transactions on Power Systems, vol. 30, no. 3, pp. 1195-1202, 2014.
38. M. S. Jahan and N. Amjady, "Solution of large-scale security constrained optimal power flow by a new bi-level optimisation approach based on enhanced gravitational search algorithm," IET Generation, Transmission & Distribution, vol. 7, no. 12, pp. 1481-1491, 2013.
39. Q. Wang, J. D. McCalley, T. Zheng, and E. Litvinov, "Solving corrective risk-based security-constrained optimal power flow with Lagrangian relaxation and Benders decomposition," International Journal of Electrical Power & Energy Systems, vol. 75, pp. 255-264, 2016.
40. J. Mohammadi, G. Hug, and S. Kar, "Agent-based distributed security constrained optimal power flow," IEEE Transactions on Smart Grid, vol. 9, no. 2, pp. 1118-1130, 2016.
41. H. Yu and W. Rosehart, "An optimal power flow algorithm to achieve robust operation considering load and renewable generation uncertainties," IEEE Transactions on Power Systems, vol. 27, no. 4, pp. 1808-1817, 2012.
42. A. Venzke, D. T. Viola, J. Mermet-Guyennet, G. S. Misyris, and S. Chatzivasileiadis, "Neural Networks for Encoding Dynamic Security-Constrained Optimal Power Flow to Mixed-Integer Linear Programs," arXiv preprint arXiv:2003.07939, 2020.
43. M. Velay, M. Vinyals, Y. Besanger, and N. Retière, "Fully distributed security constrained optimal power flow with primary frequency control," International Journal of Electrical Power & Energy Systems, vol. 110, pp. 536-547, 2019.
44. A. J. Wood, B. F. Wollenberg, and G. B. Sheblé, Power generation, operation, and control. John Wiley & Sons, 2013.
45. H. R. Nikzad and H. Abdi, "A robust unit commitment based on GA-PL strategy by applying TOAT and considering emission costs and energy storage systems," Electric Power Systems Research, vol. 180, p. 106154, 2020.
46. H. Abdi, H. Fattahi, and S. Lumbreras, "What metaheuristic solves the economic dispatch faster? A comparative case study," Electrical Engineering, vol. 100, no. 4, pp. 2825-2837, 2018.
47. "The IEEE 14 BUS data." http://www.ee.washington.edu/research/pstca/ (accessed).